Acta Crystallographica Section D
Biological Crystallography
ISSN 0907-4449

Structure of a calcium-deficient form of influenza virus neuraminidase: implications for substrate binding

Brian J. Smith,[a]*‡ Trevor Huyton,[a]‡ Robbie P. Joosten,[a] Jennifer L. McKimm-Breschkin,[b] Jian-Guo Zhang,[a] Cindy S. Luo,[a] Mei-Zhen Lou,[a] Nikolaos E. Labrou[c] and Thomas P. J. Garrett[a]*

[a]The Walter and Eliza Hall Institute of Medical Research, 1G Royal Parade, Parkville, Victoria 3050, Australia, [b]CSIRO, Division of Molecular and Health Technologies, 343 Royal Parade, Parkville, Victoria 3052, Australia, and [c]Laboratory of Enzyme Technology, Department of Agricultural Biotechnology, Agricultural University of Athens, Iera Odos 75, 11855 Athens, Greece

‡ These authors contributed equally.

Correspondence e-mail: bsmith@wehi.edu.au, tgarrett@wehi.edu.au

Received 3 April 2006
Accepted 29 May 2006

PDB Reference: influenza virus neuraminidase, 2b8h, r2b8hsf.

The X-ray structure of influenza virus neuraminidase (NA) isolated from whale, subtype N9, has been determined at 2.2 Å resolution and contains a tetrameric protein in the asymmetric unit. In structures of NA determined previously, a calcium ion is observed to coordinate amino acids near the substrate-binding site. In three of the NA monomers determined here this calcium is absent, resulting in structural alterations near the substrate-binding site. These changes affect the conformation of residues that participate in several key interactions between the enzyme and substrate and provide at a molecular level the basis of the structural and functional role of calcium in substrate and inhibitor binding. Several sulfate ions were identified in complex with the protein. These are located in the active site, occupying the space reserved for the substrate (sialic acid) carboxylate, and in positions leading away from the substrate-binding site. These sites offer a new opportunity for the design of inhibitors of influenza virus NA.

1. Introduction

Influenza infection has been a major threat to public health throughout the world for centuries. Some pandemics such as the 1917–1919 'Spanish flu' were responsible for the deaths of tens of millions of people throughout the world. Vaccination remains the primary method for prevention of influenza, but vaccine strains must be continually updated and their protective efficacy is limited in patients beyond 65 years of age, the major target group (Nicholson *et al.*, 2003). An alternative lies in antiviral drugs. Influenza neuraminidase (NA) has been proven as a valid therapeutic target for antiviral drugs owing to its essential role in the viral replication cycle (Lamb, 1989; Colman, 1994). NA is thought to enhance viral mobility *via* hydrolysis of the α-(2,3)- or α-(2,6)-glycosidic linkage between a terminal sialic acid (Neu5Ac) residue and its adjacent carbohydrate moiety on the host receptor. These molecules with terminal Neu5Ac are also the target receptors for the viral haemagglutinin (HA; Ward, 1981), the major surface glycoprotein on the viral particle surface. NA destroys these HA receptors, allowing progeny virus particles, budding from infected cell surfaces, to be released (Palese *et al.*, 1974).

The functional NA exists as a tetramer of identical subunits. The NA tetramer forms a box-like head on top of a long stalk domain and is anchored in the viral membrane by a hydrophobic sequence near the N-terminus. The surface of an influenza virus typically has about 50 tetrameric NA spikes (Murti & Webster, 1986), with each spike displaying fourfold rotational symmetry. The NA active site has been characterized as a strain-invariant cavity on the upper surface of each NA subunit (Varghese & Colman, 1991). The protein fold consists of a symmetric arrangement of six four-stranded

Table 1
Data-collection statistics and refinement.

Values in parentheses are for the outer shell.

Data collection	
Resolution range (Å)	20–2.2 (2.28–2.20)
Total No. of observations	680297
No. of independent reflections	115894
R_{merge}	0.086 (0.366)
Completeness (%)	99.7 (97.8)
Mean $I/\sigma(I)$	16.3 (4.6)
Crystal parameters	
Space group	$P3_221$
Unit-cell parameters (Å, °)	$a = b = 107.52$, $c = 338.49$, $\alpha = \beta = 90$, $\gamma = 120$
Refinement	
Resolution range (Å)	20–2.2 (2.26–2.20)
No. of reflections (working set)	110050
No. of reflections (free set)	5806
R_{free}	0.189 (0.225)
R_{cryst}	0.139 (0.149)
R.m.s. deviation from ideality	
Bonds (Å)	0.023
Angles (°)	2.0
No. of atoms (tetrameric unit, excluding hydrogen)	
Protein (including carbohydrate)	12829
Water	1367
Glycerol	18 (3 molecule)
Sulfate	150 (30 molecules)
Chloride	4

antiparallel β-sheets arranged as the blades of a propeller. There is a calcium-binding site connected to the active site *via* conserved residues. The functional role of calcium in the structure is unknown, although calcium has been shown to be necessary for NA activity (Chong *et al.*, 1991; Johansson & Brett, 2003) and it is essential for the thermostability of the protein (Burmeister *et al.*, 1994).

We report here the structure of influenza virus NA isolated from whale. While the structure of whale N9 NA in complex with antibody has been reported previously (Malby *et al.*, 1994), the structure described here is of a tetrameric form in which three of the monomers do not have the high-affinity calcium-binding site occupied. Changes in conformation of residues normally in complex with a calcium ion cause structural alterations in residues that bind substrate and inhibitors. The crystallization conditions contain sulfate in high concentration, resulting in several sulfate ions being observed in complex with the protein.

2. Materials and methods

2.1. Protein expression and purification

The A/NWS/whale/Maine/1/84 (H1N9) reassortant influenza virus (P05803) was originally obtained from Dr R. Webster (Memphis, TN, USA) and was grown in eggs for isolation of NA. NA was removed by two successive treatments with 1 mg ml^{-1} pronase (Calbiochem) to yield the head domain (from the stalk) at 310 K for 2.5 h and purified by gel-filtration chromatography as previously reported (McKimm-Breschkin *et al.*, 1991).

2.2. Crystallization

The purified N9 NA isolated from whale was initially used to deglycosylate an unrelated mammalian cell-surface receptor. The receptor was treated with NA and purified using a size-exclusion column that was intended to separate the NA from the receptor. Initially, very small crystals grew out of a heavy precipitate (presumed to be the mammalian receptor) in conditions identified using commercial sparse-matrix screens (Hampton Research). The best crystals grew by hanging-drop vapor diffusion by equilibrating a 1 µl drop of protein in buffer (10 m*M* HEPES pH 7.2, 50 m*M* ammonium sulfate) with 1 µl reservoir solution containing 2.0–2.5 *M* ammonium sulfate and suspended over 1 ml reservoir solution. Small cube-shaped crystals grew to maximum dimensions of $\sim 50 \times 50 \times 50$ µm over 3–12 months. For data collection, crystals were harvested in stabilization solution containing 10% more precipitant (2.2–2.7 *M* ammonium sulfate) before transfer to a cryoprotectant solution consisting of stabilization solution with 30%(*v*/*v*) glycerol. Crystals were then mounted in a nylon loop and flash-cooled directly into liquid nitrogen.

2.3. X-ray crystallography

High-resolution diffraction data (to 2.2 Å) were collected on a Quantum-4 CCD detector (Area Detector Systems Corp.) at beamline 14-BM-C, Advanced Photon Source, Chicago, IL, USA. Data processing was performed with *HKL* (Otwinowski & Minor, 1997). The structure was solved by MIR using the program *SOLVE* (Terwilliger & Eisenberg, 1983, 1987; Terwilliger *et al.*, 1987; Terwilliger & Berendzen, 1996, 1999) from data collected on uranyl acetate and platinum iodide derivatives (data not shown). Density modification and NCS averaging with the program *RESOLVE* (Terwilliger, 2002) permitted identification of the polypeptide backbone chain. At this point we could clearly see the β-propeller fold characteristic of NA, which was not consistent with the expected receptor. Closer inspection by superposition of tern N9 NA (PDB code 7*nn*9) with *LSQMAN* (Kleywegt & Jones, 1994) on the partially built structure showed a close fit with the experimental map.

2.4. Structure calculation

The structure of the head domain of whale N9 NA (residues 82–469) was resolved by molecular replacement using the program *AMoRe* with the tern N9 NA as a search model. The sequence of whale N9 NA is 97% identical to that of the model (tern), differing in the following amino acid substitutions: D83E, K187R, T188A, H233Q, A269T, R284Q, E286G, I287V, R304Q, V358G, K387R, D457N. The sequence of whale N9 NA here differs from that reported earlier (Air *et al.*, 1987) at residue 157; in the structure determined in the present study this residue, at the interface between NA monomers, is an alanine. Following rigid-body refinement with *REFMAC*5 (Murshudov *et al.*, 1999) and simulated annealing in *CNS* (Brünger *et al.*, 1998), manual rebuilding was performed using *O* (Jones *et al.*, 1991). Final refinement using NCS restraints was then performed with *REFMAC*5. Statistics for the final

model are presented in Table 1. The structure was validated using the program *WHATCHECK* (Hooft *et al.*, 1996). The final model has 82% of the residues in the most favoured region of the Ramachandran plot and one residue in the disallowed region (but well fitted to the electron density).

3. Results and discussion

Crystals of whale N9 NA were obtained serendipitously during attempts to crystallize an unrelated protein. NA had been used to desialylate the target protein of similar size. Subsequent purification by size-exclusion chromatography had not removed all the NA and resulted in trace amounts of NA in the crystallization medium. Crystals from this medium were identified as NA and possessed features not observed in the structures of NA determined previously. In particular, a highly conserved calcium ion was absent in three of the monomers of the tetramer and sulfate ions were observed in and near the enzyme active site.

The crystal form of whale N9 NA reported here contains one tetramer in the asymmetric unit in space group $P3_221$, with a V_M of 3.1 Å^3 Da^{-1} (Matthews, 1968). Earlier crystallization studies of whale N9 NA also yielded one tetramer in the asymmetric unit in space group $P2_12_12_1$ at 3.0 Å resolution from high-phosphate buffer conditions, with a V_M of 4.7 Å^3 Da^{-1} (Taylor *et al.*, 1993).

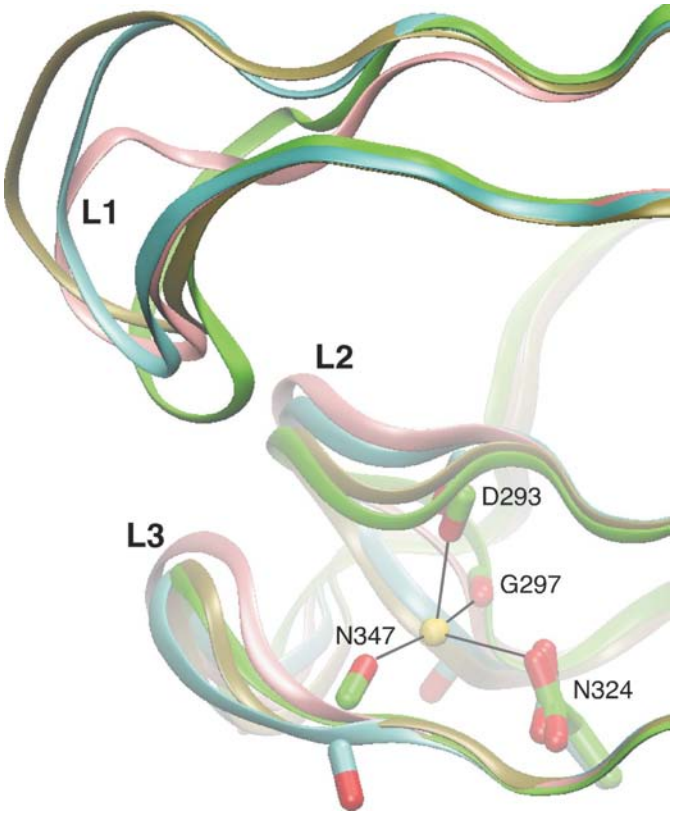

Figure 1
Ribbon diagram of the calcium-binding site and structural changes between calcium-bound (green, chain *A*) and calcium-free (cyan, chain *B*; pink, chain *C*; tan, chain *D*) forms of NA. The loops L1 (245–251), L2 (295–298) and L3 (343–344) adopt different conformations in the four monomers. In the calcium-bound form, the protein backbone carbonyl O atoms of Asp293, Gly297 and Asn347 and the side-chain carboxylate of Asp324 all bind the calcium cation (yellow sphere). In the calcium-free form of chain *B*, the carbonyl groups of Gly297 and Asn347 are shown to be flipped from the conformation observed in the calcium-bound form.

3.1. High-affinity calcium-binding site

The structure of whale N9 NA determined here contains one whole tetramer in the asymmetric unit (monomers *A*–*D*). Each monomeric unit of whale N9 NA closely resembles the structure of tern N9. In tern N9 a calcium ion binds several electronegative atoms, including the protein backbone carbonyl O atoms of Asp293, Gly297 and Asn347 and the carboxylate side chain of Asp324. In whale N9 NA, however, this ion does not appear to be present in each of the monomers. In the *A* monomer of whale N9 NA a small cation (electron density equivalent to a sodium or magnesium ion) draws each of the groups above into the same orientation as that observed in tern NA. Notably, the identity of this ion has been unambiguously resolved in N8 by microPIXE experiments (Taylor *et al.*, 1993) to be calcium. In monomers *B*, *C* and *D*, however, this ion is absent. To alleviate the potential electrostatic repulsion between the atoms that would otherwise bind the cation, a reorientation of the groups in this region is observed, resulting in a change in the position of residues in the loops Ser245–Asp251 (L1), Trp295–Ser298 (L2) and Gly343–Asn344 (L3). The path of the polypeptide chain in these loops is different in each of the calcium-deficient monomers (Fig. 1); by comparison, the paths of the polypeptide chains outside these loops of all monomers, *A*–*D*, are identical (*i.e.* the root-mean-square deviation in backbone-atom positions in the superposition of each monomer ranges from 0.21 to 0.30 Å). In each of the monomers *B*–*D* several of the loops L1–L3 participate in the formation of crystal contacts, but not in monomer *A*. The contacts differ for each monomer, leading to heterogeneity of the loop conformations (Fig. 1). The ability of these loops to adopt alternative conformations indicates an inherent flexibility of these loops in the absence of calcium and explains the sensitivity toward proteases in the absence of calcium (Burmeister *et al.*, 1994).

Superposition of the structures of monomer *A* of whale N9 NA determined here and that previously determined in complex with NC10 antibody (Malby *et al.*, 1994; PDB code 1nmb) yields an r.m.s.d. of 0.34 Å. In the structure of whale N9 NA–antibody complex the calcium ion was thought to be present. However, both tern N9 and this complex were crystallized from buffer with potassium phosphate at high concentration (1.7 *M*). In the antibody complex the L3 loop of NA contacts the antibody; specifically, the amide carbonyl of Gly343 and the side chain of Asn344 of NA form hydrogen bonds with the side chain of Thr93 (on the third light-chain CDR) of the antibody. In monomers *B*–*D* in which the calcium is absent, the alteration in loop configuration would preclude the interaction involving Gly343 in a complex with antibody, while the interaction with Asn344 could be maintained.

The active site of influenza A NA may be divided into five subsites (AS1–AS5; Stoll *et al.*, 2003). Subsite 1 (AS1), is

formed by three arginine residues, Arg118, Arg292 and Arg371, and binds the substrate carboxylate group. AS2 is a negatively charged region of the active site, formed by Glu119 and Glu227; this site accommodates the guanidinium group of zanamivir or the ammonium group of oseltamivir. AS3 has hydrophobic residues and contains the side chains of Trp178 and Ile222 and anchors the *N*-acetyl group of sialic acid, oseltamivir and zanamivir. AS4 is a hydrophobic region that does not directly participate in binding substrate. AS5 is comprised of the carboxylate of Glu276 and the methyl group of Ala246.

In AS5, the neuraminidase subtypes N2 (Varghese *et al.*, 1992) and N9 (Varghese *et al.*, 1997) bind substrate with the carboxylate of Glu276 in a *trans* conformation (with respect to the $C_\beta-C_\gamma$ bond) and hydrogen bonded to the hydroxyl groups O8 and O9 of sialic acid (Fig. 2*a*); the guanidinium group of Arg224 forms a bidentate interaction with the carboxyl group of Glu276. The side chain of Glu276 can exist in a *gauche* conformation forming an alternative bidentate-bridging interaction with Arg224 (Fig. 2*b*). With Glu276 in this conformation, AS5 presents a hydrophobic environment. Only when Glu276 adopts this *gauche* conformation can the enzyme bind inhibitors such as the carboxamide derivatives of zanamivir (Taylor *et al.*, 1998), oseltamivir (Varghese *et al.*, 1998) or BCX-1812 from Biocryst Pharmaceuticals (Babu *et al.*, 2000; Smith *et al.*, 2002). In the N6 subtype of neuraminidase (E. Rudino-Pinera, P. Tunnah, S. J. Crennell, R. G. Webster, W. G. Laver & E. F. Garman, unpublished results; PDB codes 1v0z, 1w20, 1w21), Glu276 adopts a *gauche* conformation that is still capable of forming a hydrogen bond with O9 of sialic acid, but not O8. The trace of the polypeptide chain of N6 differs from the calcium-associated form of N9 significantly in the loop connecting the last strand of β-sheet 4 and the first strand of β-sheet 5 (Varghese *et al.*, 1983), from Pro342 to Asn347 (Thr348 to Pro346 in N6), containing the loop L3. Notably, the structure of N6 shows a calcium ion in an identical position as observed in N9. In all monomers of whale N9 NA, Glu276 adopts the *gauche* conformation, forming a bidentate-bridging interaction with Arg224, as observed in the ligand-free form of N6 NA (E. Rudino-Pinera, P. Tunnah, S. J. Crennell, R. G. Webster, W. G. Laver & E. F. Garman, unpublished results; PDB codes 1v0z, 1w20, 1w21).

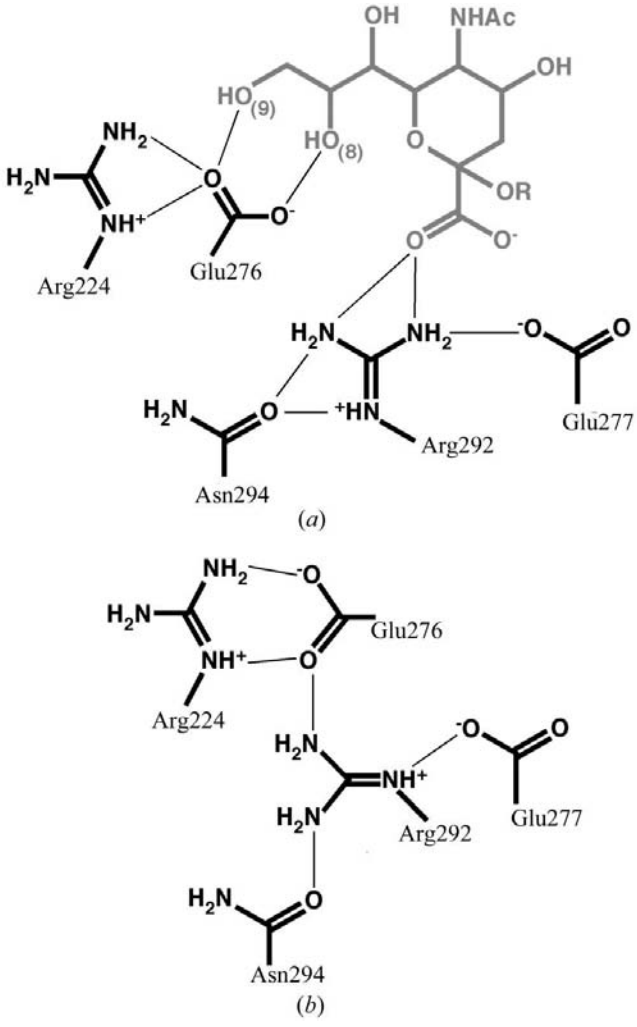

Figure 2
The structural differences between chains *A* and *B* in the vicinity of the substrate-binding site. (*a*) Substrate, sialic acid (grey), is normally coordinated at the carboxylate by Arg292 and at the glycerol by Glu276. (*b*) Structural alterations in chain *B* prevent binding to substrate. Substrate-binding residues Glu276 and Arg292 are sequestered into positions unable to bind ligand.

In AS1, a triad of arginine residues complexes the carboxylate of the substrate sialic acid. The side chain of these three residues is usually fully extended in the many structures of neuraminidases and *trans*-sialidases determined to date. In the *B* monomer of whale N9 NA, Arg292 adopts an unusual conformation, folding back toward Asn294. The side chain of Arg292 forms a hydrogen bond with the side-chain carbonyl O atom of Asn294 despite significant movement of the L2 loop caused by the absence of the stabilizing calcium ion in this monomer. In this conformation, the guanidinium group of Arg292 forms hydrogen bonds with Glu276, Glu277 and Asn294 (Fig. 2*b*). In the other three monomers (*A*, *C* and *D*) the conformation of the side chain of Arg292 is fully extended, forming hydrogen bonds with Glu277 and Asn294.

The R292K mutant of N9 posses an altered sensitivity to inhibitors with replacement of the substrate glycerol, such as oseltamivir or BCX-1812 (Varghese *et al.*, 1998; Smith *et al.*, 2002). This reduced inhibitory activity presumably results from an increased energy requirement for the conformational change of Glu276 required to accommodate such inhibitors. In this mutant the lysine side chain does not extend to the carboxylate group of these inhibitors or the substrate and lacks a pair of hydrogen bonds between ligand and enzyme normally associated with this residue (Arg292). Notably, the R292K mutant of N9 has only 20% of the specific activity of wild-type N9 and is associated with significant drug resistance (Varghese *et al.*, 1998).

Calcium ions are known to control the rate of interaction of substrate with the enzyme and the strength of association of inhibitors (Chong *et al.*, 1991). Activation of NA by calcium had been proposed to occur through a conformational change in the active site. The structure of whale N9 NA determined

here shows that Arg292 and Glu276 adopt altered conformations in a calcium deficient form of the enzyme. If these conformational changes are maintained upon ligand binding, then the number of hydrogen bonds to the ligand is reduced substantially, presumably resulting in reduced affinity of the enzyme for the ligand. Alternatively, the energy required to present these residues in a 'native' conformation (*i.e.* one in which calcium is present), will result in reduced binding to the ligand.

3.2. Sulfate-binding sites

During model refinement, several large features were observed in the electron-density maps. In the $F_o - F_c$ difference density the intensity of these peaks ranged between 24σ and 6σ and possessed clear tetrahedral morphology. Attempts to model these features as water resulted in unacceptable residuals in the $F_o - F_c$ difference density. The intensity of these features and the presence of sulfate in high concentration in the crystallization medium allowed us to unambiguously identify these as sulfate ions.

The sequestering of Arg292 in a conformation unable to bind ligand occurs in only one of four monomers of whale N9 NA. In the other three monomers a sulfate ion holds the side chain of Arg292 in an extended conformation (Fig. 3). In each of the monomers a sulfate ion was observed situated in the position usually occupied by the substrate's carboxylate moiety (sulfate-binding subsite 1; SBS1), where it forms ionic interactions with the side-chain guanidinium groups of the arginine residues 118, 292 and 371. One of the O atoms of this sulfate anion also comes into close contact with a carboxylate O atom of Asp151 (~3.2 Å). Two of the sulfate O atoms occupy the same position as a pair of water molecules

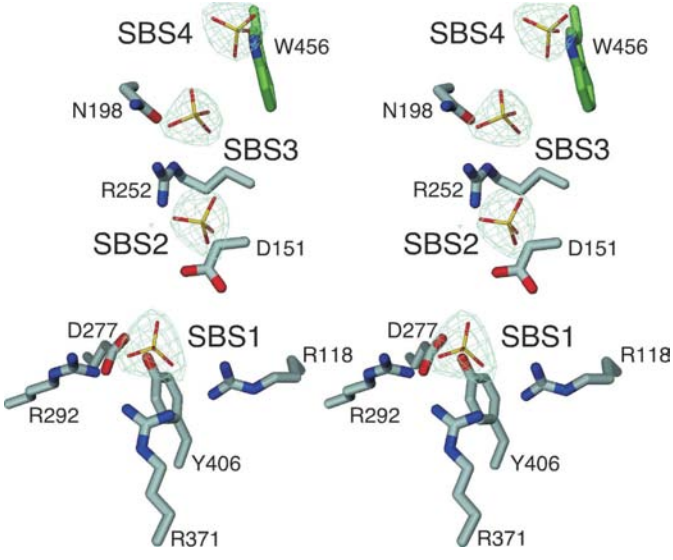

Figure 3
Stereoview of the sulfate-binding sites SBS1–4 of whale N9 NA as observed in the 2.2 Å crystal structure. Electron density from a refined OMIT map (contoured at the 3.5σ level) about the sulfate ions with tetrahedral form shows their position. Sulfate anions are presented as thin tubes and the side chains of active-site residues are displayed as heavy tubes.

observed in a high-resolution (1.80 Å) structure of N9 (Varghese *et al.*, 1995).

Lying close to Asp151, but outside the substrate-binding site, is a second sulfate anion that forms a hydrogen bond with the $N_{\delta1}$ atom of His150 (SBS2). The distance of closest approach between the carboxylate O atom of the side chain of Asp151 and an O atom of this sulfate falls in the range 2.71–3.41 Å in the four monomers; these distances are consistent with a neutral carboxyl group (Vilminot *et al.*, 1974; Cano & Martínez-Carrera, 1974; Vilminot & Philippot, 1976; Capasso *et al.*, 1983; Nagashima *et al.*, 1992; Srinivasan *et al.*, 2001*a*,*b*). Sequence analysis of clinical isolates of influenza virus have identified Asp151 as the most variable of the conserved residues (McKimm-Breschkin *et al.*, 2003); substitution by residues incapable of acting as an acid (asparagine, valine and glycine), however, deny Asp151 a critical role in catalysis.

Extending further from the binding site are two more sulfates (SBS3 and SBS4), the first interacting with the side-chain atoms of Arg152 and Asn198, and the second forming a hydrogen bond with the N_ε of Trp456 from a neighboring monomer. Together, these four ions form a string of sulfates extending from the binding site, with S atoms 6.0–7.6 Å apart.

Crystal structures of influenza virus neuraminidases have been determined on many previous occasions in the presence and absence of ligand. In many cases the medium used for crystallization required high phosphate concentrations [although the crystallization of Tokyo N2 (Varghese *et al.*, 1992) and N6 (Taylor *et al.*, 1993) do not require high phosphate]. However, phosphate ions have not been observed in any of these structures. Sulfate ions, presumably, have a higher affinity for NA, particularly the SBSs 1–4, than phosphate ions. At the pH of the crystallization medium (pH 6–7) phosphate ions are predominantly in a −1 charge state, while sulfate ions are almost exclusively in a −2 charge state. It would appear that the SBSs may have highest affinity for ions in a −2 charge state. This would also account for the low affinity of the substrate and inhibitor carboxylate, with −1 charge, in a calcium-deficient enzyme.

This is the first time that the sulfate-binding sites of influenza virus NA have been identified and therefore offer a new opportunity for ligand design targeted against influenza virus. The residues that form SBS1–3 are associated with generally conserved residues, although clinical isolates have been identified with mutations in residues Arg292, Asp151 and Arg152 (McKimm-Breschkin *et al.*, 2003), each contributing to one or more of these SBSs. Recently, we have utilized this information in the design of non-carbohydrate-based inhibitors of NA (Platis *et al.*, 2006). Benzylsulfonates based on the polysulfonate triazine dye Cibacron Blue 3 GA were shown to be potent inhibitors of NA (K_i = 0.13 μ*M*).

4. Conclusions

The high-resolution crystal structure of influenza virus N9 neuraminidase isolated from whale has been solved in the presence of sulfate. The structure is essentially identical to the structures solved previously, with two exceptions. A calcium

ion that draws several electronegative groups together in the earlier structures is missing in three of the monomeric units of the tetrameric assembly of the structure presented here. The absence of this ion causes a disruption in the conformation of several loops surrounding the calcium-binding site, causing structural changes in the substrate-binding site. These changes in conformation can account for the requirement for calcium ions for enzyme activity and stability.

Sulfate ions occupying sites in and around the substrate-binding site were clearly identified in the structure. The affinity of charged species for these sites may provide utility in the design of ligands, as potential inhibitors or diagnostics, against influenza virus neuraminidase.

This work was supported by the NHMRC and the Australian Synchrotron Research Program. Use of the BioCARS sector at the Advanced Photon Source was also supported by the NIH National Center for Research Resources and the US Department of Energy. We are grateful to P. M. Colman for helpful discussions.

References

Air, G. M., Webster, R. G., Colman, P. M. & Laver, W. G. (1987). *Virology*, **160**, 346–351.
Babu, Y.S., Chand, P., Bantia, S., Kotian, P., Dehghani, A., El-Kattan, Y., Lin, T.-H., Hutchison, T. L., Elliot, A. J., Parker, C. D., Sandya, L. A., Horn, L. L., Laver, G. W. & Montgomery, J. A. (2000). *J. Med. Chem.* **43**, 3482–3486.
Brünger, A. T., Adams, P. D., Clore, G. M., DeLano, W. L., Gros, P., Grosse-Kunstleve, R. W., Jiang, J.-S., Kuszewski, J., Nigles, M., Pannu, N. S., Read, R. J., Rice, L. M., Simonson, T. & Warren, G. L. (1998). *Acta Cryst.* D**54**, 905–921.
Burmeister, W. P., Cusack, S. & Ruigrok, R. W. H. (1994). *J. Gen. Virol. 75*, 381–388.
Cano, F. H. & Martínez-Carrera, S. (1974). *Acta Cryst.* B**30**, 2729–2732.
Capasso, S., Mattia, C. A., Mazzarela, L. & Zagari, A. (1983). *Acta Cryst.* C**39**, 281–283.
Chong, A. K. J., Pegg, M. S. & von Itzstein, M. (1991). *Biochim. Biophys. Acta*, **1077**, 65–71.
Colman, P. M. (1994). *Protein Sci.* **3**, 1687–1696.
Hooft, R. W. W., Vriend, G., Sander, C. & Abola, E. E. (1996). *Nature (London)*, **381**, 272.
Johansson, B. E. & Brett, I. C. (2003). *J. Biochem.* **134**, 345–352.
Jones, T. A., Zou, J. Y., Cowan, S. W. & Kjeldgaard, M. (1991). *Acta Cryst.* A**47**, 110–119.
Kleywegt, G. J. & Jones, T. A. (1994). *Jnt CCP4/ESF–EACBM Newsl. Protein Crystallogr.* **31**, 9–14.
Lamb, R. A. (1989). *The Influenza Viruses*, edited by R. M. Krug, pp. 1–87. New York: Plenum.
McKimm-Breschkin, J. L., Caldwell, J. B., Guthrie, R. E. & Kortt, A. A. (1991). *J. Virol. Methods*, **32**, 121–124.
McKimm-Breschkin, J., Trivedi, T., Hampson, A., Hay, A., Klimov, A., Tashiro, M., Hayden, F. & Zambon, M. (2003). *Antimicrob. Agents Chemother.* **47**, 2264–2272.
Malby, R. L., Tulip, W. R., Harley, V. R., McKimm-Breschkin, J. L., Laver, W. G., Webster, R. G., & Colman, P. M. (1994). *Structure*, **2**, 733–746.
Matthews. B. W. (1968). *J. Mol. Biol.* **33**, 491–497.
Murshudov, G. N., Lebedev, A., Vagin, A. A., Wilson, K. S. & Dodson, E. J. (1999). *Acta Cryst.* D**55**, 247–255.
Murti, K. G. & Webster, R. G. (1986). *Virology*, **149**, 36–43.
Nagashima, N., Sano, C., Kawakita, T. & Iitaka, Y. (1992). *Anal. Sci.* **8**, 723–725.
Nicholson, K. G., Wood, J. & Zambon, M. (2003). *Lancet*, **362**, 1733–1745.
Otwinowski, Z. & Minor, W. (1997). *Methods Enzymol.* **276**, 307–326.
Palese, P., Tobita, K., Ueda, M. & Compans, R. W. (1974). *Virology*, **61**, 397–410.
Platis, D., Smith, B. J., Huyton, T. & Labrou, N. E. (2006). In the press.
Smith, B. J., McKimm-Breschkin, J. L., McDonald, M., Fernley, R. T., Varghese, J. N. & Colman, P. M. (2002). *J. Med. Chem.* **45**, 2207–2212.
Srinivasan, N., Sridhar, B. & Rajaram, R. K. (2001*a*). *Acta Cryst.* E**57**, o679–o681.
Srinivasan, N., Sridhar, B. & Rajaram, R. K. (2001*b*). *Acta Cryst.* E**57**, o772–o774.
Stoll, V., Stewart, K. D., Maring, C. J., Muchmore, S., Giranda, V., Gu, Y.-G., Wang, G., Chen, Y., Sun, M., Zhao, C., Kennedy, A. L., Madigan, D. L., Xu, Y., Saldivar, A., Kati, W., Laver, G., Sowin, T., Sham, H. L., Greer, J. & Kempf, D. (2003). *Biochemistry*, **42**, 718–727.
Taylor, N. R., Cleasby, A., Singh, O., Skarzynski, T., Wonocott, A. J., Smith, P. W., Sollis, S. L., Howes, P. D., Cherry, P. C., Bethell, R., Colman, P. M. & Varghese, J. (1998). *J. Med. Chem.* **41**, 798–807.
Taylor, G., Garman, E., Webster, R., Saito, T. & Laver, G. (1993) *J. Mol. Biol.* 230, 345–348.
Terwilliger, T. C. (2002). *Acta Cryst.* D**58**, 2213–2215.
Terwilliger, T. C. & Berendzen, J. (1996). *Acta Cryst.* D**52**, 749–757.
Terwilliger, T. C. & Berendzen, J. (1999). *Acta Cryst.* D**55**, 849–861.
Terwilliger, T. C. & Eisenberg, D. (1983). *Acta Cryst.* A**39**, 813–817.
Terwilliger, T. C. & Eisenberg, D. (1987). *Acta Cryst.* A**43**, 6–13.
Terwilliger, T. C., Kim, S.-H. & Eisenberg, D. (1987). *Acta Cryst.* A**43**, 1–5.
Varghese, J. N. & Colman, P. M. (1991). *J. Mol. Biol.* **221**, 473–486.
Varghese, J. N., Colman, P. M., van Donkelaar, A., Blick, T. J., Sahasrabudeh, A. & McKimm-Breschkin, J. L. (1997). *Proc. Natl Acad. Sci. USA*, **94**, 11808–11812.
Varghese, J. N., Epa, V. C. & Colman, P. M. (1995). *Protein Sci.* **4**, 1081–1087.
Varghese, J. N., Laver, W. G. & Colman, P. M. (1983). *Nature (London)*, **303**, 35–40.
Varghese, J. N., McKimm-Breschkin, J. L., Caldwell, J. B., Kortt, A. A. & Colman, P. M. (1992). *Proteins*, **14**, 327–332.
Varghese, J. N., Smith, P. W., Sollis, S. L., Blick, T. J., Sahasrabudhe, A., McKimm-Breschkin, J. L. & Colman, P. M. (1998). *Structure*, **6**, 735–746.
Vilminot, P. S. & Philippot, E. (1976). *Acta Cryst.* B**32**, 1817–1822.
Vilminot, P. S., Philippot, E. & Cot, L. (1974). *Acta Cryst.* B**30**, 2602–2606.
Ward, C. W. (1981). *Curr. Top. Microbiol. Immunol.* **94–95**, 1–74.